JVI Journals.ASM.org

Morphology, Physiological Characteristics, and Complete Sequence of Marine Bacteriophage ϕRIO-1 Infecting *Pseudoalteromonas marina*

Stephen C. Hardies,[a] Yeon J. Hwang,[b] Chung Y. Hwang,[c] Gwang I. Jang,[b] Byung C. Cho[b]

Department of Biochemistry, The University of Texas Health Science Center at San Antonio, San Antonio, Texas, USA[a]; Microbial Oceanography Laboratory, School of Earth and Environmental Sciences, and Research Institute of Oceanography (RIO), Seoul National University, Seoul, South Korea[b]; Division of Life Sciences, Korea Polar Research Institute, Incheon, South Korea[c]

Bacteria of the genus *Pseudoalteromonas* are ubiquitous in the world's oceans. Marine bacteria have been posited to be associated with a major ancient branch of podoviruses related to T7. Yet, although *Pseudoalteromonas* phages belonging to the *Corticoviridae* and the *Siphoviridae* and prophages belonging to the *Myoviridae* have been reported, no *Pseudoalteromonas* podovirus was previously known. Here, a new lytic *Pseudoalteromonas marina* phage, ϕRIO-1, belonging to the *Podoviridae* was isolated and characterized with respect to morphology, genomic sequence, and biological properties. Its major encoded proteins were distantly similar to those of T7. The most similar previously sequenced viruses were *Pseudomonas* phage PA11 and *Salinivibrio* phage CW02. Whereas many elements of the morphology and gene organization of ϕRIO-1 are similar to those of podoviruses broadly related to T7, ϕRIO-1 conspicuously lacked an RNA polymerase gene. Since definitions of a T7 supergroup have included similarity in the DNA polymerase gene, a detailed phylogenetic analysis was conducted, and two major DNA polymerase clades in *Autographivirinae* and several structural variants of the *polA* family represented in podoviruses were found. ϕRIO-1 carries an operon similar to that in a few other podoviruses predicted to specify activities related to γ-glutamyl amide linkages and/or unusual peptide bonds. Most growth properties of ϕRIO-1 were typical of T7-like phages, except for a long latent period.

Viral particles outnumber bacteria in the world's oceans by a factor of about 10:1 and are thought to enforce diversity at the base of the microbiological community by restraining overgrowth of any particularly successful microbial species and returning their biomolecules as nutrients into the water through lysis (1, 2). This role rests critically on a network of specific host-virus interactions. Estimates of viral diversity by metagenomics tend to indicate extraordinarily high numbers of viral species (3–5), yet the total number of sequenced marine bacteriophages as of the last published count (6) was only 17. Current marine phage sequencing initiatives are expected to raise this to only a few hundred.

Two of the earliest marine phages genomically characterized were the podoviruses roseophage SIO1 (7) and vibriophage VpV262 (8). These exemplify a group of podoviruses that are vaguely similar to enterobacterial phage T7 but lack the single-chain RNA polymerase and have two converging transcription units rather than one unidirectional transcription unit. It was postulated that this description represented an ancestral phage type present in ancient oceans and widespread descendants would be found in oceanic bacterial species.

Pseudoalteromonas is a genus of gammaproteobacteria with many species, all found in marine environments. The genus contains specialists for various marine habitats ranging from sea ice (9) to deep-sea sediments (10). Its species are divided into pigmented and nonpigmented species; the former are known for habitation of marine biofilms and production of antimicrobial and algicidal substances, while the latter are found living dispersed in the water column (11). The specific host isolate discussed here was isolated from open seawater and is of the latter variety. *Pseudoalteromonas* phages isolated thus far include ϕPM2, a phage with a small double-stranded circular DNA genome and lipid-containing virion which is the type phage for the family *Corticoviridae* (12), and ϕH105/1, a siphovirus (13). Genomic characterization has also indicated the presence of myoviral prophages (13). In this study, we address the apparent absence of podoviruses infecting *Pseudoalteromonas* by isolating and characterizing ϕRIO-1, a podovirus infecting a specific isolate of *Pseudoalteromonas marina*.

The genome of ϕRIO-1 was analyzed for its relationships to other known podoviruses and its mosaicism versus that of the other known podoviruses. Its most closely related relatives are *Pseudomonas* phage PA11 (14) and *Salinivibrio* phage CW02 (15). It contains a suite of genes that have predicted activities related to synthesizing and breaking unusual peptide linkages, first discussed by Iyer et al. (16) as possibly being involved in modifying cell wall metabolism, and that are more fully described here. These genes are shared in a variable fashion with PA11 and CW02 as well as with the LUZ24-like podoviruses (17). ϕRIO-1 is like SIO1 and VpV262 in genomic organization and has genes with divergent similarity to the T7 structure and morphogenesis genes, as well as the gene for the divergent T7-like DNA polymerase first described for SIO1. We looked more extensively at the DNA polymerase due to the proposal that it is a marker of T7-related phages in general (7). We further looked at variation in the thumb domain, following up on the observation that the T7 DNA polymerase had evolved a processivity domain on the tip of the thumb (18).

Received 5 June 2013 Accepted 6 June 2013
Published ahead of print 12 June 2013
Address correspondence to Byung C. Cho, bccho@snu.ac.kr, or Stephen C. Hardies, hardies@uthscsa.edu.

doi:10.1128/JVI.01521-13

MATERIALS AND METHODS

Seawater samples. The seawater samples from which both ϕRIO-1 and its host strain, CL-E25, were isolated were collected on 10 December 2007 in the East Sea, South Korea (37°54′20″N, 128°49′50″E, 8.4°C, 33.2 practical salinity units).

Bacterial strains. The host isolation strain, designated CL-E25, was colony purified on marine agar (Difco) plates. After PCR amplification with rRNA gene primers 27F and 1492R (19) and DNA sequencing, the 16S rRNA gene of CL-E25 was found to be identical to that of *Pseudoalteromonas marina* mano4^T (KCTC 12242^T). *Pseudoalteromonas marina* mano4^T and other strains for host range determination were either obtained from the Korean Collection for Type Cultures (KCTC) or isolated from various marine environments.

Phage isolation. Seawater was filtered through 0.22-μm-pore-size membranes (Millipore), and phages were concentrated using Amicon Ultra-15 centrifugal filter units (Millipore). After spot testing showed lytic activity against CL-E25, phages were amplified in a liquid culture of CL-E25, and ϕRIO-1 was isolated by four rounds of plaque purification.

Transmission electron microscopy. The morphology of ϕRIO-1 was examined after negative staining with 2% uranyl acetate by energy-filtering transmission electron microscopy (LIBRA 120; Carl Zeiss, Germany) at 120 kV at NICEM (Seoul, South Korea).

Biological characterization. All plaque assays were performed with a 0.4% agar overlay on marine agar at 25°C, with plaque development occurring in 1 day, and assays were conducted in triplicate. For thermal or pH stability measurements, phage at a starting concentration of 10^8 PFU/ml in marine broth (Difco) was held under the indicated conditions for 1 h before titers were determined. Chemical sensitivity was tested as described previously (20). Briefly, the chemical solvent was mixed with phage at 10^9 PFU/ml at the indicated ratio, and the mixture was held at 25°C with shaking for 1 h. After centrifugation in the case of immiscible solvents, the organic solvent was removed by evaporation overnight at 4°C. Burst size, latent time, and adsorption rates were determined as described previously (21). For burst size and latent time, the phages were preadsorbed for 10 min at 25°C; then, unadsorbed phages were removed by three washes with 1-min spins, and the adsorbed cells were diluted to 50 volumes. The effect of temperature on phage production was determined as described previously (22). Briefly, 10^5 cells were infected at a multiplicity of infection of 0.1, incubated at room temperature for 20 min, and then grown at the indicated temperature for 6 h prior to determination of the titer.

Purification of phage and viral nucleic acids. Phages were purified from a 1-liter overnight culture. Bacteria were removed by centrifugation, followed by filtering through a 0.22-μm-pore-size membrane (Millipore). Phages were concentrated using Amicon Ultra-15 centrifugal filter units (Millipore). Purification was as described previously (23), using a CsCl step gradient (35,000 rpm, 3 h, SW 41 Ti rotor). The phage band was desalted, put into SM buffer (100 mM NaCl, 8 mM $MgSO_4$, 50 mM Tris at pH 7.5) using Amicon Ultra-15 centrifugal filter units (Millipore), and stored at 4°C. Viral DNA was prepared as described previously (24), using proteinase K digestion in sodium dodecyl sulfate, followed by phenol-chloroform-isoamyl alcohol extraction and ethanol precipitation.

Genome characterization. The genome size was first estimated by pulsed-field gel electrophoresis (CHEF DRIII; Bio-Rad). The genome was subjected to shotgun sequencing at Macrogen (Seoul, South Korea). Restriction mapping with SspI, BssHII, and FspI was initially used to approximately locate the position of the terminal repeats that had overlapped to produce the circular sequence. Subsequently, a ligation product of blunt-ended vector and intact viral DNA was PCR amplified to provide template for sequencing the exact left and right ends.

Bioinformatic analysis. Open reading frames (ORFs) were predicted using a combination of GeneMark (25) and Glimmer (26) software. Even very short frames were annotated if they fit reasonably between other frames and had good ribosome binding site predictions. Hence, the possibility of missing frames was minimized at the cost of possibly tolerating some false-positive frame predictions. Translated ORFs were analyzed through PsiBlast, rpsblast, hmmer3, and hhpred searches as previously described (27). Mobile introns and tRNA genes were excluded through Rfam (28) and tRNAScan (29) searches. Graphic analysis among the most closely related phages was carried out using the b36chain program (27) and was then followed up with dot plot analysis with NCBI's blast-two-sequences tool. b36chain finds distant protein similarities by calculating a relaxed E value reflecting the likelihood of finding a weak blast match in the same position relative to surrounding well-matching domains. Dot plot analysis allows detection of even weaker similarity using a visual impression of the matching intensity on the long diagonal to the noise matches scattered off the long diagonal as its significance filter. BLASTP bit scores for tabulating patterns of similarity across genomes were derived from a combination of local searches with the NCBI blast tool kit and use of the NCBI blast-two-sequences online tool.

A global alignment of the DNA polymerase sequences including the thumb domain required special procedures because we could find no multiple-sequence-alignment program that would align all the sequences at once all the way through the thumb domain and generate results consistent with the available structural alignments. DNA polymerase alignments within closely related groups were carried out using a local implementation of the sequence alignment and modeling system (30). To align among groups, each group alignment was converted to an hhpred-style hidden Markov model, and model-to-model alignment was carried out using a local implementation of the hhsearch software (31). The bacterial polymerase with Protein Data Bank (PDB) accession number 3PO4 (32) and its relatives were found to have the minimal structure. Each group of sequences was first aligned to the sequences of the members of the family with PDB accession number 3PO4 using hhsearch. Insertions relative to the sequence with PDB accession number 3PO4 were manually deleted from each group alignment, and then the groups were put into a global alignment. Comparison of the structural alignments of the T7 sequence to the mitochondrial sequence or the T7 sequence to the sequence with PDB accession number 3PO4 made in this fashion was performed, and the sequences were judged to have no more than 10% of residues out of alignment, mostly as a result of arbitrary decisions about which residues should begin or end a given insert. The alignment with the insert states thus removed is available from the corresponding authors. The tree was created with PAUP (33) using neighbor joining with 100 cycles of bootstrap analysis. The tree was collapsed to a consensus at the 85% bootstrap support level, except for the branch relating cellular to phage polymerases, which was left at 78%.

Nucleotide sequence accession number. The annotated sequence has been deposited in GenBank with accession number KC751414.

RESULTS

Host range and plaque morphology. As a strategy to increase the range of phages that might be cultured, both the isolation host and phage ϕRIO-1 were derived from the same seawater sample. Subsequent host range determination (Table 1) indicated that ϕRIO-1 is highly specific for its locally derived isolation host. ϕRIO-1 would not even plate on *P. marina* mano4^T, which is the *Pseudoalteromonas* type strain to which the isolation host CL-E25 exhibited a perfect 16S rRNA gene match. Hence, plating of seawater samples against preconceived type strains only would underestimate the diversity of coadapted host-phage pairs occurring in the marine environment. The plaque morphology (Fig. 1A) consists of a clear center with a turbid halo surrounded by a clear halo.

Biological properties. The ambient seawater temperature in the region where the phage was found fluctuates from 2.2°C in winter to 24.7°C in summer. Temperature and pH survival curves (Fig. 2) indicated that ϕRIO-1 has excellent survival up to 30°C and a relatively narrow pH optimum of about 7. Therefore, the

TABLE 1 Host range of phage ϕRIO-1

Indicator host	Pigmented	Plaque
Pseudoalteromonas marina (CL-E25P)	−	+
Pseudoalteromonas marina^T (= KCTC 12242^T)	−	−
Pseudoalteromonas translucida (CL-AS1)	−	−
Pseudoalteromonas arctica (CL-A10)	−	−
Pseudoalteromonas atlantica (CL-ES1)	−	−
Pseudoalteromonas paragorgicola (CL-E22)	−	−
Pseudoalteromonas paragorgicola (CL-E31)	−	−
Pseudoalteromonas phenolica (CL-TW1)	+	−
Pseudoalteromonas nigrifaciens (CL-100D-75-1)	+	−
Pseudoalteromonas nigrifaciens (CL-100D-75-3)	+	−
Pseudoalteromonas nigrifaciens (CL-D75-3)	+	−
Alteromonas macleodii (CL-A1)		−
Alteromonas macleodii (CL-East 21a)		−
Alteromonas marina (CL-East 21)		−
Alteromonas tagae (CL-East 47)		−
Idiomarina fontislapidosi (CL-MA6)		−
Idiomarina loihiensis (CL-I1)		−

phage presumably can range far to the south. Liquid growth experiments (Fig. 3) also indicated that the phage and host have good growth properties through the range of summer temperatures. At 10°C, phage production was reduced by 2 orders of magnitude, but the phage was clearly able to propagate in rich medium. The phage was found to be stable against exposure to chloroform and diethyl ether but not acetone or ethanol. The phage pseudo-first-order adsorption constant was $\sim 7 \times 10^{-9}$ ml/min. This is close to the estimated diffusion-limited rate (34). One-step growth curves conducted at 25°C indicated a burst size of 118 ± 8, a latent period of 60 min, and rise of 30 min. These

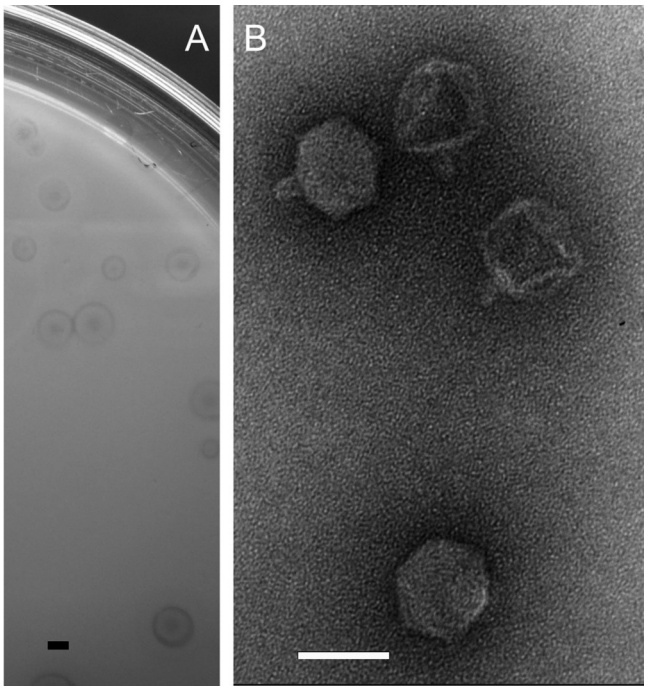

FIG 1 (A) Plaque morphology of ϕRIO-1; (B) electron micrograph of ϕRIO-1. Bars, 1 mm (A) and 50 nm (B).

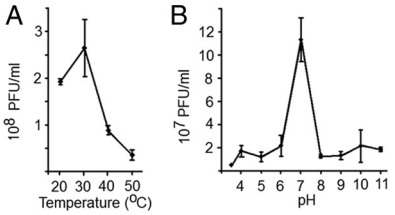

FIG 2 Stability of ϕRIO-1. (A) Temperature; (B) pH.

numbers are typical of podoviruses with typical laboratory hosts grown at 37°C, except for a lengthened latent period.

Phage morphology. Electron microscopy of ϕRIO-1 revealed the classic form of a T7-like podovirus with an icosahedral head of 51 nm in diameter and a short tail of 15 nm in length and 12 nm in width (Fig. 1B). Phages sharing that morphology include phages of the subfamily *Autographivirinae*, including T7, SP6, and ϕKMV, as well other podoviruses (35). The goal of the sequence analysis was therefore to clarify the relationships of ϕRIO-1 to these and other podoviruses, including marine phages SIO1 and VpV262.

Genomic characterization. The ϕRIO-1 genome was sequenced with 10.5-fold coverage and found to be 43,882 bp long, including 121-bp direct terminal repeats at a fixed genomic position. The G+C content was 44.7% without any major blocks of sequence deviating from the average. This compares to a host genomic composition with a G+C content of 39.6%. Open reading frames were predicted, and functional assignments were made (Fig. 4) using the variety of profile sequence searching methods listed in Materials and Methods. The genome was organized into two converging transcription units. Inferred functions related to structure and morphogenesis versus host takeover, replication, and lysis appeared to segregate cleanly into the right and left arms, respectively, in the orientation depicted. Phage ϕRIO-1 exhibited essentially no BLASTN matches to any other genomes. To bring out its organizational relationships to other phages, its sequence was graphically aligned using sensitive protein-protein matching based on positionally biased BLASTP searches (27). In comparison to standard blast and family database searches, this method provides additional capabilities to discover the similarities of individual genes as well as to discover the descent or exchange of multigene modules. An example of how each of these capabilities improves the understanding of the ϕRIO-1 genome is given below.

An example of the positionally biased search used to predict the function of a gene occurs with *orf22* and *orf23*, just downstream of the encoded DNA polymerase. The sequences of the prospective translation products of these two ORFs do not match any se-

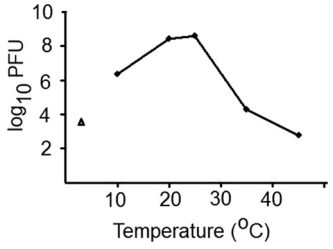

FIG 3 Phage production at different temperatures. Triangle, initial titer.

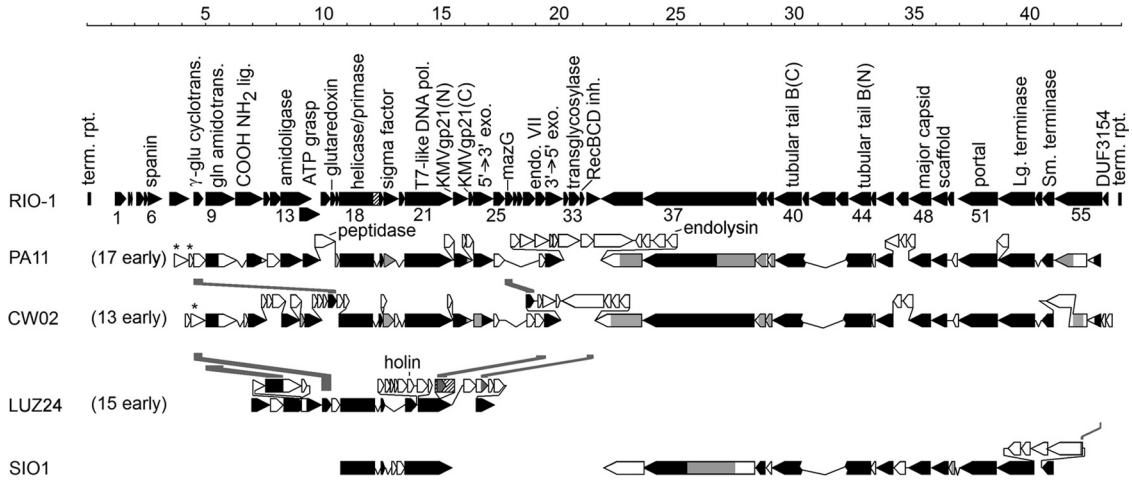

FIG 4 Comparative genomic organizations of phages similar to ϕRIO-1. The scale is in kilobases. Abbreviations for labeled features are as follows: term. rpt., terminal repeat; cyclotrans., cyclotransferase; amidotrans., amidotransferase; lig., ligase; pol., polymerase; exo., exonuclease; endo., endonuclease; inh., inhibitor; Lg., large; Sm., small. The organizations of other phages with genes of similar sequence are drawn under the positions of their proposed ϕRIO-1 homologs and shaded as follow: black, a positionally biased BLASTP match found by a phage versus a phage b36chain search (27); gray, an extended similarity found by gene-versus-gene dot plot matching. Open glyphs do not have sequence similarity to ϕRIO-1 in any non-profile-based search strategy. Glyphs raised above the main track of glyphs indicate a longer sequence relative to ϕRIO-1, and a triangular dipping line indicates a shorter sequence than in ϕRIO-1. Diagonally hatched features are group I introns. Three additional genes annotated as amidotransferases in PA11 and CW02 are marked with asterisks. All genes are indicated for PA11 and CW02, except for the indicated number of small presumptive early genes. Only matches are shown for LUZ24 and SIO1. The SIO1 genome map includes revisions in assembly and annotation previously suggested (8).

quences in the protein databases by BLASTP or any profile family database search. Indeed, by the criteria used in many annotation pipelines, one or both of these would not be annotated as open reading frames at all. In the positionally biased search regimen, the fact that there were well-matched proteins encoded by PA11 (14) to the left and right of these frames caused a BLASTP search to be conducted with a database size reduced to just a few PA11 proteins encoded by genes in that area. This resulted in significant E values for a match indicating that these two ORFs are a broken version of a PA11 gene found at the same genomic position. The improved E value should be understood to be conditional on the assertion that this string of genes, including the DNA polymerase on the left and the exonuclease on the right, descended as a module from a common ancestral phage operon. Subsequent exploration of the PA11 gene revealed it to be a member of a protein family found downstream of the DNA polymerase in many podoviruses and indicated to be members of the ϕKMVgp21 family in Fig. 4. The ϕKMVgp21 family has been encountered many times before but has never been assigned any function by sequence similarity. With the additional sequences now available to join its sequence profile, after multiple rounds of PsiBlast we now find similarity to single-stranded DNA binding protein.

Besides aiding in the functional identification of individual genes, the positionally biased search algorithm can string together multigene matches while skipping over insertions or deletions. Graphing the strings of matched genes brings out the prospective common ancestry of multigene modules. The matched genes and inserted or deleted segments are depicted by the string of glyphs in Fig. 4. Only two other phages were found that could be considered to have shared a common ancestor end to end with intervening insertions and deletions. These were *Pseudomonas* phage PA11 (14) and *Salinivibrio* phage CW02 (15). The method was also used to explore the relationship of ϕRIO-1 to the two marine phages SIO1 and VpV262, which are known to be organized similarly to each other but have greatly divergent replicative genes (8). ϕRIO-1 was matched broadly to both SIO1 and VpV262 in the structure and morphogenesis region but only to SIO1 in the replicative region. Only the genes of SIO1 are shown in Fig. 4. The match of ϕRIO-1 to PA11 and CW02 differs from its match to SIO1 by extensive matching to genes to the left of the DNA helicase and polymerase genes in PA11 and CW02. That particular novel module of genes was also found in the LUZ24-like phages (17), genes for the type phage of which are shown in Fig. 4.

Criteria for functional assignments. For the following encoded proteins, functional predictions were ultimately based on similarity to proteins of known function encoded by T7. The helicase/primase, DNA polymerase (including its 3′ → 5′ exonuclease domain), and the stand-alone 5′ → 3′ exonuclease could be confidently matched to T7 simply by a BLASTP search of the NCBI nr database. The major structure and morphogenesis functions, capsid protein, portal, tail tube B, and large terminase subunit were eventually matched to T7 proteins but required multiple rounds of PsiBlast to do so. Many of the other functions were assigned on the basis of protein family database matches. In a few cases, the link to a protein family first required linking to a protein in another phage by the positionally biased BLASTP approach, as described above for the homolog of ϕKMVgp21. Similar circumstances occurred for the predicted sigma factor and for the predicted COOH-NH_2 ligase. Finally, a few genes were annotated using a criterion other than pure sequence similarity. The scaffold function was assigned due to its coiled coil content and the universality of its position in T7-related head structure modules and because PsiBlast was able to detect sequence similarity with other presumptive scaffold proteins encoded in this position in the more closely related phages. The gene for small terminase was assigned on the basis of two properties typically found for small terminase genes in other phages. One was that it is usually close to the gene for large terminase. The other was that it is usually con-

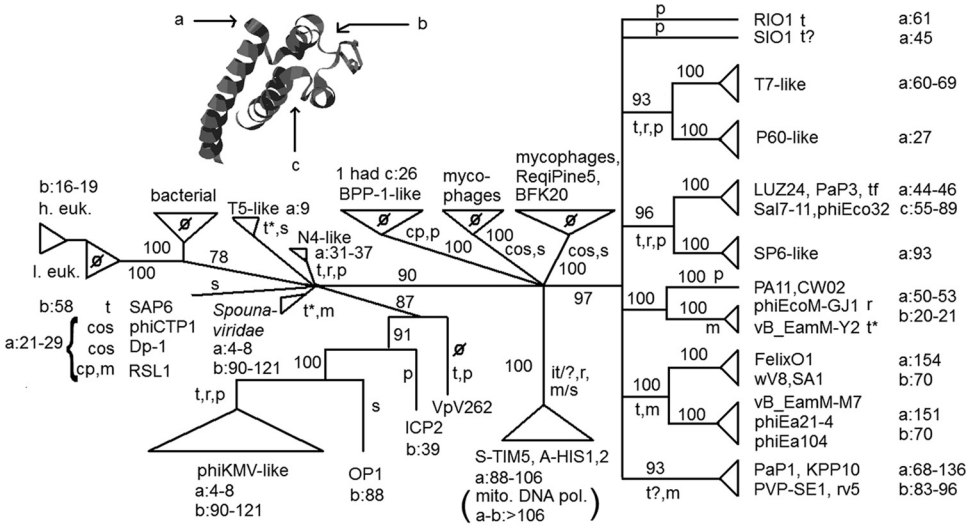

FIG 5 Tree relating the descent of the *polA* polymerases with structural changes in the thumb and distribution into different phages. Numbers on the branches are bootstrap values. The root is presumed to be on one end or the other of the link between cellular and phage polymerases at the upper left, depending on whether one imagines that phage polymerase was derived from cellular polymerase, or vice versa. The selection of bacterial polymerases used to represent cellular *polA* genes was from COG079 in the Cluster of Orthologous Groups (COG) database. The selection of eukaryotic polymerases used was from the theta polymerase family. h. euk., higher eukaryotes (animals including sea urchins and above); l. euk., lower eukaryotes (plants and animals below sea urchins). Mitochondrial DNA polymerases (mito. DNA pol.), in parentheses, were not included in the tree-making computation but are marked on the figure in the position previously determined (39). Each phage is labeled as to family (p, podovirus; s, siphovirus; m, myovirus) either individually or on a branch leading to a group. The types of ends observed or inferred in each group are indicated as follows: t, short fixed terminal repeats; t*, long fixed terminal repeats; cp, circularly permuted; it, inverted fixed terminal repeats; cos, cohesive ends. r, the presence of a T7-related single-chain RNA polymerase in a phage or group of phages. The inset at the upper left shows the thumb domain from the sequence with PDB accession number 3PO4 (a typical bacterial *polA* polymerase). a, b, and c, three interhelical regions in which inserted sequences are observed in the phage polymerase alignment. The range of insert sizes in each region is indicated near each group. The symbol ø emphasizes that a group is essentially devoid of inserts in the thumb.

served in at least some number of closely related phages. *orf54* was the only gene meeting those criteria. *orf6* was predicted to encode a spanin, according to its content of predicted transmembrane helices on both the N and C termini with an appropriate length to span from the inner to the outer membrane (36).

Phylogenetic and systematic relationships of ϕRIO-1. An early concept about how to classify podoviruses put weight on the relatedness of the DNA polymerase (7). Later concepts put weight on the relationships of a greater number of proteins (8) or on multiple proteins but with special reference to the presence or absence of the single-chain RNA polymerase (35). The relatedness of the major ϕRIO-1 proteins was examined as follows:

(i) DNA polymerase. An alignment of essentially all *polA* polymerases was produced, and their sequence relationships are summarized in a molecular phylogenetic tree (Fig. 5). The root is presumed to be on one end or the other of the link between cellular and phage polymerases at the upper left, depending on whether one imagines that phage polymerase was derived from cellular polymerase, or vice versa. Due to the idea that SIO1 plus T7 and possibly other podoviruses might be clustered as a subset of podoviruses on the basis of DNA polymerase similarity, the family affiliation (podo-, myo-, or siphovirus) was marked for each clade. Clearly, by the divergence time separating SIO1 and ϕRIO-1 from T7, the DNA polymerase has exchanged between podoviruses and myoviruses.

In consideration of the observation that T7 DNA polymerase has a processivity domain on the tip of the thumb domain relative to bacterial DNA polymerase I (pol I) (18), we asked if that might be a common feature distinguishing phage-encoded *polA* polymerases from cellular *polA* polymerases. To ask that question, the sequences were aligned through the thumb region using special procedures (see Materials and Methods). Including the thumb domain did not materially alter the tree topology, but it did clarify the presence or absence and position of thumb domain inserts in each of the clades of the tree. The bacterial *polA* polymerases were indeed devoid of inserts in the thumb domain. Eukaryotic nuclear *polA* polymerases were devoid of thumb domain inserts, except for a late-arising clade. Eukaryotic mitochondrial *polA* polymerases, which are thought to have been phage derived (37), are known from crystal structure analysis (38) to have large thumb domain inserts. The phages most similar to mitochondrial *polA* polymerases, A-HIS1 and -2 and S-TIM5 (39, 40), also have insertions in that position. Not all phage clades had thumb inserts. Those that did have inserts in the thumb often had inserts of different sizes and/or inserts in places different from the locations observed in T7 DNA polymerase. The location and size ranges of the inserts in the phage clades are indicated in Fig. 5. Also, in an attempt to correlate the thumb inserts with other functions, we indicated the presence or absence of phage-encoded RNA polymerase and the type of genome ends in each clade of Fig. 5.

(ii) Global relationships among the podoviruses. The current subfamily classification within podoviruses groups ϕKMV-like phages with T7-, SP6-, and P60-like phages into the subfamily *Autographivirinae*. The grouping is based on the content of a gene for single-chain RNA polymerase and some degree of similarity of the proteome to T7 (35). Therefore, the finding that ϕRIO-1 and SIO1 DNA polymerases were relatively close to the T7 DNA polymerase but that the ϕKMV DNA polymerase was far away was

TABLE 2 BLASTP bit scores among major proteins of selected podoviruses

Phages compared	BLASTP bit score							
	RNAP	Helicase	DNA polymerase	5′ → 3′ exonuclease	Tail tube B	Capsid	Portal	Terminase
T7 and gh-1	1,001	568	786	207	882	385	731	672
T7 and Syn5	228	262	218	73	175	69	282	410
T7 and ϕKMV	259	<20[a]	44	<20	**160**	**30**	**187**	**240**
ϕRIO-1 and ϕKMV		<20	27	**46**	<20	<20	22	37
ϕRIO-1 and T7		**104**	**172**	28	<20	<20	<20	<20
ϕRIO-1 and CW02		308	143	157	172	198	323	317
ϕRIO-1 and PA11		349	138	164	150	196	312	328
PA11 and CW02		511	714	208	553	398	511	837

[a] For weakly matching proteins, the stringency of BLASTP was reduced until at least one high-scoring segment pair was reported. If the reported high-scoring segment pair was not consistent with the alignment established by PsiBlast, it was regarded as noise and a value of <20 was entered. This value represents the average bit score associated with noise in these searches.

somewhat surprising. We asked if the DNA polymerase was unusual in this respect or if the other large well-conserved members of the ϕRIO-1 proteome clustered with T7 relative to ϕKMV. In order to explore this issue, the BLASTP bit scores of the other proteins that were large enough and conserved enough to have a measurable bit score among T7, ϕRIO-1, and ϕKMV were tabulated (Table 2). The three central rows of Table 2 give the results of the three-way comparison among ϕRIO-1, T7, and ϕKMV, with the strongest matches given in bold. It can be seen that the mosaicism is more complex than just the DNA polymerase gene being incongruent with the other genes. The order of genes tabulated corresponds to their order in the ϕRIO-1 genome. The structure and morphogenesis genes generally show a closer relationship between T7 and ϕKMV, as might be expected from their inclusion in a common subfamily. However, the helicase/primase function shows a relationship in which ϕRIO-1 is closer to T7, much like the DNA polymerase. The clustering of genes with these two patterns suggests a recombination involving a replicative multigene module and a structure and morphogenesis multigene module.

In between the major replicative genes and the structure/morphogenesis module, a single gene predicted to encode a 5′ → 3′ exonuclease showed yet again a different relationship, in which ϕRIO-1 and ϕKMV were the closest. We asked if this was a singular instance or if there might be a module of neighboring genes with a more recent ϕRIO-1/ϕKMV common ancestor in the right part of the replicative module. One such case includes the two preceding ORFs, which, as mentioned above, encode a broken and diverged version of ϕKMVgp21 and for which there is generally an intact well-conserved version of that gene in ϕRIO-1's closest relatives (Fig. 4). As mentioned above, the ϕKMVgp21 family is now thought to be a family of single-stranded DNA binding proteins. As such, ϕKMVgp21 is an alternative to the T7 single-stranded DNA binding protein gene. Indeed, ϕKMVgp21 members appear in podoviral genomes lacking the more T7-like single-stranded DNA binding protein, and most podoviruses have a gene from one or the other of these two families.

A further connection to ϕKMV in this region was found in *orf30*. This gene encodes a protein similar to the endonuclease VII recombination junction resolvase found in ϕKMV-like phages and in some other T7-related phages but not in T7 itself or ϕRIO-1's closest relatives. There is some confusion about the role of endonuclease VII stemming from examples like that noted in LUZ24 (Fig. 4), wherein the endonuclease VII gene is carried in a group I intron in the fashion of a homing endonuclease. Nonetheless, endonuclease VII is a structural homolog of the T7 endonuclease I resolvase and so may also be considered a ϕKMV-related alternative to a T7 function. Finally, the inferred stand-alone 3′ → 5′ exonuclease encoded by *orf31* is the only ϕRIO-1 protein easily matched to a ϕKMV protein by BLASTP. This predicted 3′ → 5′ exonuclease is in addition to the 3′ → 5′ exonuclease domain fused to the DNA polymerase. There is no second T7-encoded stand-alone 3′ → 5′ exonuclease. Hence, there is potentially a module from *orf22* to *orf31* which has the most recent common ancestry between ϕRIO-1 and ϕKMV and for which the T7 versions of the contained functions are not clustered.

To support consideration of how ϕRIO-1 should be classified, additional lines were added to Table 2. The two phages PA11 and CW02, found to be organized like ϕRIO-1 (Fig. 4), were also found to be most similar to ϕRIO-1 in each of the tabulated genes. PA11 and CW02 were consistently closer to each other than to ϕRIO-1 (Table 2, bottom three rows). Hence, there are no broad-scale modular exchanges in evidence in the descent of these three phages since their common ancestor. To give some sense of scale for these relationships, we also tabulated the relationship between T7 and the most divergent of the phages formally included within the T7-like phage genus, *Pseudomonas* phage gh-1 (41). The relationship between PA11 and CW02 was at a level of divergence similar to that between T7 and gh-1. As an example of a phage previously studied in comparison to T7 and at a level of divergence similar to that between ϕRIO-1 and CW02, the P60-like phage Syn5 was listed (42). Hence, the ancestor to the ϕRIO-1/CW02/PA11 group was at a level of divergence outside the genus level for the T7-like phages but within the range assigned to the subfamily *Autographivirinae*.

Finally, we looked at the divergence relationships in the novel module in *orf8* through *orf14* (Table 3). As elsewhere in the genome, PA11 and CW02 were consistently closer than ϕRIO-1 and CW02. The relationship to LUZ24 was much further away.

DISCUSSION

In this study, a new lytic phage infecting the marine bacterium *Pseudoalteromonas marina* was characterized. According to the morphological and genomic features, ϕRIO-1 is a member of the family *Podoviridae*. For most of its proteins, the most similar sequence match to a heavily characterized prototypical virus was to T7, but these matches typically required several rounds of PsiBlast

TABLE 3 BLASTP bit scores relating the proteins of the putative peptidoglycan modification operon

Phages compared	BLASTP bit score				
	Cyclotransferase	Amidotransferase	COOH-NH_2 ligase	Amidoligase	ATP grasp enzyme
PA11 and CW02	NA[a]	156	264	169	247
ϕRIO1-CW02	70	131	72	71	212
ϕRIO1-LUZ24	58	114	65	57	87

[a] NA, not applicable.

to discover. ϕRIO-1's closest sequenced relatives are *Pseudomonas* phage PA11 and *Salinivibrio* phage CW02. The established measure for grouping podoviruses into a genus is 40% of proteins matching within a 75 bit score by BLASTP (35). The relationship of ϕRIO-1 to any phage is outside that threshold (e.g., 25% to PA11). The divergence values of individual ϕRIO-1 proteins were also beyond the greatest divergence observed within the established T7-like phage genus (Table 2). However, we have shown that there are no broad-scale modular exchanges in the descent from the common ancestor of ϕRIO-1, CW02, and PA11. Hence, their respective biological properties should be similar, except in those areas commonly modulated by single gene exchanges. Hence, we suggest stretching the numerical criterion and putting ϕRIO-1, CW02, and PA11 into a single genus in the spirit that classification should reflect commonality of biological properties.

In their broader relationships, the ϕRIO-1-like phages are mosaic, and it becomes necessary to think of the similarity of the sequence and function of individual modules or clusters of genes rather than of the genome as a whole. They lack a single-chain RNA polymerase, share a novel early or intermediate gene module with the LUZ24-like phages, and have major replicative functions most like those of T7-like phages but auxiliary replicative and recombination functions more like those of ϕKMV-like phages. ϕRIO-1 does not have a well-defined lysis module. There is a potential endolysin encoded by *orf33* in a region where lysis functions tend to be scattered in related phages (Fig. 4). However, a clear holin gene has not yet been identified, and the spanin appears to be placed in an unusual location with the early genes. The structure and morphogenesis module is a version of the podoviral form more divergent than that clustered within the *Autographivirinae* (essentially T7 to ϕKMV).

Putative peptidoglycan modification module. Perhaps the most interesting of the modules in the ϕRIO-1-like phages is the novel collection of genes inferred to encode activities relating to synthesizing unusual peptide bonds or carrying out chemistry on γ-glutamyl groups (*orf8* to *orf14*). That those genes are engaged in some common pathway is suggested by the observation that they are conserved, with some variation in the position, domain organization, and number of genes, in a series of other phages: enterobacterial phage ϕEco32 (43), *Salmonella* phage 7-11 (44), *Pseudomonas* phages PA11 (14), tf (45), MR299-2 (46), LUZ24, and PaP3 (47), and *Salinivibrio* phage CW02 (15). Iyer et al. (16), commenting on three of these genes in ϕEco32, proposed that they functioned to modify the cell wall. This proposal was based on the observation that the three inferred activities, γ-glutamyl amidoligase, another amidoligase, and the ATP grasp enzyme, are appropriate to synthesize three of the unusual peptide linkages in the peptidoglycan peptide side chain. The purpose of the phage-directed synthesis was posited to be prevention of superinfection.

However, the hypothesis was advanced only in consideration of ϕEco32, which was believed to be a temperate phage wherein the residence of a prophage over host generations would permit synthesis of a substantial portion of the cellular peptidoglycan. Phages ϕRIO-1, LUZ24, tf, and others that conserve this operon are believed to be purely lytic phages. So, to keep the peptidoglycan synthesis hypothesis alive would require some purpose that could benefit a lytic phage during its brief stay in the cell. We could suggest that perhaps the minimal amount of peptidoglycan that turns over during a lytic cycle is replaced with a phage-directed version to ensure sites for the phage-borne endolysin to act or to otherwise weaken the cell wall in preparation for lysis.

Besides noting the conservation of the module in lytic phages, the other observation that we can add is the linkage of two additional functions with the putative synthetic enzymes, a predicted γ-glutamyl cyclotransferase and a glutamine amidotransferase. γ-Glutamyl cyclotransferases are always associated with the breakdown of γ-glutamate linkages through formation of a cyclic intermediate. Of the three characterized subgroups of γ-glutamyl cyclotransferases (48), ϕRIO-1 gp8 belongs to the third subgroup, which is bacterial. This subgroup is not well characterized as to its function, but one member is known to remove a γ-glutamic acid by cyclization from a moiety analogous to an ε-lysine during synthesis of an antibiotic (49). Iyer et al. (16) further noted the frequent clustering within the genome of a bacterial γ-glutamyl cyclotransferase gene with a glutamine amidotransferase gene, positing a coupling of these two activities to perform some metabolic function. They also noted that when amidotransferases are not clustered with a cyclotransferase, they were instead clustered with a peptidase. The phage genomes (Fig. 4) also exhibited this dichotomy of the function clustered with the amidotransferases. In most of the phages, the clustered gene encoded a cyclotransferase, but in PA11, there was instead a peptidase encoded immediately after the ATP grasp gene.

Amidotransferases generally transfer an amide group from the γ group of glutamine. The acceptor of the phage proteins is not predictable from the sequence. The phage-borne members are most similar to fructose-6-phosphate transaminases in the N-terminal domain, and some phage-borne members have been misannotated with that designation, but the phage-borne enzymes clearly are not similar to the C-terminal domains that bind fructose-6-phosphate. Curiously, the number of annotated amidotransferases among the related phages is variable, with PA11 having three of them. When there are multiple amidotransferases, they are of divergent families, indicating some long-standing functional specialization. At least some of them, e.g., PA11 gp1, match well to family models of both amidotransferase and peptidase_C26 (Pfam accession no. PF07722), indicating that it is possible that an amidotransferase can be a γ-linked peptide bond peptidase in disguise. This opens the door to the theory that the

function collaborated upon by the cyclotransferase and amidotransferases may be degradative instead of synthetic.

In addition to the phages that are discussed here, one other phage, Marvin (50), encodes an amidotransferase and an amidoligase that are separately derived from host genomes. That suggests that the function embodied in the cyclotransferase and amidotransferase is not just coincidentally associated with the cluster of amidoligases and the ATP grasp enzyme in ϕRIO-1-related phages. If the proposition of involvement of the synthetic functions in cell wall synthesis is correct, then the two additional activities could be posited to catalyze some additional modification to the phage-directed peptidoglycan. Alternatively, one could imagine these two activities being involved in intercepting the host-synthesized peptidoglycan monomer and truncating its peptide to allow the phage enzymes to conduct replacement synthesis.

While the peptidoglycan modification hypothesis is attractive in that it explains the coordinated retention of three enzymes that synthesize unusual peptide bonds, we caution that alternative functions have not been ruled out for this cluster of genes. Some of the enzymes could be involved in recovering from the cell wall amino acids resulting from either turnover of the host cell wall or cannibalism of surrounding cell debris. An exploration of the cellular cyclotransferases supports such a role. The number of bacterial cyclotransferase genes per bacterial genome is variable, with a high of 15 found in the genome of *Haliangium ochraceum* DSM 1436 (51). *H. ochraceum* is a scavenger of other bacteria, which might explain a need for degrading a variety of different peptidoglycan cross-linkages. However, an alternative, that the multiple cyclotransferase genes are distributed into *Haliangium orcharceum* on an as yet uncharacterized prophage, has not been excluded. Finally, it would be difficult to dismiss the possibility that any or all of these enzymes are involved in host takeover by modifying or reversing modification of host enzymes.

Main replication module. Figure 5 produced the surprise not only that ϕKMV DNA polymerase is far diverged from T7 DNA polymerase but further that the T7 polymerase processivity domain (18) was not uniformly distributed over phage *polA* polymerases. The T7 processivity domain consists of an extension from the end of the thumb that partially wraps around the newly synthesized DNA and that recruits thioredoxin to essentially act as a polymerase subunit completing a ring around the DNA. If a demand for processivity was the only thing that differentiated the use of *polA* in phages versus its role as a repair enzyme in cells, we would expect a solution of this kind to have arisen early in the phage polymerase lineage and to have been conserved thereafter. Instead, we observed numbers of different domain insertions in the phage *polA* thumb domain, which might logically be different solutions to the same problem, and numbers of phage lineages with no thumb insertions. It is, however, true that the bacterial lineage has no incidence of thumb insertions, indicating that there is no selective pressure to revise the polymerase structure so long as the polymerase is confined to its role in conducting short tracts of repair synthesis. Within the phages, we note that there is a correlation between altering the thumb domain and synthesizing fixed terminal repeats (Fig. 5). Synthesizing fixed terminal repeats requires restarting synthesis at fixed positions in the concatemer in coordination with packaging and then stopping within a limited distance. The mechanism of generating a regulated stop for end production is unknown but could logically interact with the provision to maintain processivity. In that view, it could be variability in the generation of the genomic ends that drives the structural variability of the phage *polA* polymerases.

Natural habitat of ϕRIO-1. The dynamic processes governing phage persistence in the oceanic environment have been investigated (1, 52). Phage ϕRIO-1 was isolated from 8.4°C water in winter, which introduces additional considerations of how the growth dynamics are modified to deal with the reduced metabolic activity imposed by low temperature. Host generation times of marine bacteria may be as long as a month under natural conditions (53, 54). The host strain was found to have a temperature optimum for replication at 25°C, with a doubling time of 29.2 min in rich medium, and maintained a generation time of 60 min at 10°C in rich medium (not shown). However, phage production dropped dramatically even in rich medium at 10°C. Lengthened latent periods due to poor nutrition have been termed "pseudolysogeny" (55), and such a strategy may be used by ϕRIO-1 at low temperature. The triple-zone plaques formed by ϕRIO-1 indicate some other form of complexity in its host interaction that is not understood. There is no indication from the sequence analysis that ϕRIO-1 can be temperate; hence, we do not believe that the turbid zones come from that source. Other precedented causes of turbid lysis zones include phage-borne or phage-produced enzymes that attack host extracellular polymers (56), feeding of hosts by phage metabolites (57), or lysis inhibition related to superinfection (58).

Phage ϕRIO-1 was tested against a variety of pigmented and nonpigmented *Pseudoalteromonas* species and species from related genera (Table 1). Some phages are known to infect strains within multiple genera (reviewed in reference 59). More commonly, phages are limited to species within the same genus or even a single species. The latter may reflect the degree of subdivision of the genus into species. Within the *Pseudoalteromonas* genus, the nonpigmented free-living species are a tightly related cluster by the criterion of the rRNA sequence (11) and, hence, relatively finely divided to species. Nonetheless, *P. marina* phage ϕRIO-1 has thus far not been found to form plaques on other species of *Pseudoalteromonas*. In summary, with the characterization of ϕRIO-1, we open the investigation of podoviral involvement in the host-phage network governing the free-living *Pseudoalteromonas* species in the marine environment.

ACKNOWLEDGMENTS

We thank M. Baudoux for helpful discussions on the early stage of the work.

This work was supported in part by a National Research Foundation of Korea (NRF) grant funded by the Korean government (MEST; no. 2011-0012369) and the BK21 project of the Korean government.

REFERENCES

1. **Wommack KE, Hill RT, Kessel M, Russek-Cohen E, Colwell RR.** 1992. Distribution of viruses in the Chesapeake Bay. Appl. Environ. Microbiol. **58:**2965–2970.
2. **Weinbauer MG.** 2004. Ecology of prokaryotic viruses. FEMS Microbiol. Rev. **28:**127–181.
3. **Hendrix RW.** 2003. Bacteriophage genomics. Curr. Opin. Microbiol. **6:**506–511.
4. **Angly FE, Felts B, Breitbart M, Salamon P, Edwards RA, Carlson C, Chan AM, Haynes M, Kelley S, Liu H, Mahaffy JM, Mueller JE, Nulton J, Olson R, Parsons R, Rayhawk S, Suttle CA, Rohwer F.** 2006. The marine viromes of four oceanic regions. PLoS Biol. **4:**e368. doi:10.1371/journal.pbio.0040368.
5. **Kristensen DM, Mushegian AR, Dolja VV, Koonin EV.** 2010. New

dimensions of the virus world discovered through metagenomics. Trends Microbiol. **18:**11–19.
6. **Paul JH, Sullivan MB.** 2005. Marine phage genomics: what have we learned? Curr. Opin. Biotechnol. **16:**299–307.
7. **Rohwer F, Segall A, Steward G, Seguritan V, Breitbart M, Wolven F, Azam F.** 2000. The complete genomic sequence of the marine phage roseophage SIO1 shares homology with nonmarine phages. Limnol. Oceanogr. **45:**408–418.
8. **Hardies SC, Comeau AM, Serwer P, Suttle CA.** 2003. The complete sequence of marine bacteriophage VpV262 infecting *Vibrio parahaemolyticus* indicates that an ancestral component of a T7 viral supergroup is widespread in the marine environment. Virology **310:**359–371.
9. **Bian F, Xie BB, Qin QL, Shu YL, Zhang XY, Yu Y, Chen B, Chen XL, Zhou BC, Zhang YZ.** 2012. Genome sequences of six *Pseudoalteromonas* strains isolated from arctic sea ice. J. Bacteriol. **194:**908–909.
10. **Qin QL, Li Y, Zhang YJ, Zhou ZM, Chen XL, Zhang XY, Zhou BC, Wang L, Zhang YZ.** 2011. Comparative genomics reveals a deep-sea sediment-adapted life style of *Pseudoalteromonas* sp. SM9913. ISME J. **5:**274–284.
11. **Bowman JP.** 2007. Bioactive compound synthetic capacity and ecological significance of marine bacterial genus *Pseudoalteromonas*. Mar. Drugs **5:**220–241.
12. **Mannisto RH, Kivela HM, Paulin L, Bamford DH, Bamford JK.** 1999. The complete genome sequence of PM2, the first lipid-containing bacterial virus to be isolated. Virology **262:**355–363.
13. **Duhaime MB, Wichels A, Waldmann J, Teeling H, Glöckner FO.** 2011. Ecogenomics and genome landscapes of marine *Pseudoalteromonas* phage H105/1. ISME J. **5:**107–121.
14. **Kwan T, Liu J, Dubow M, Gros P, Pelletier J.** 2006. Comparative genomic analysis of 18 *Pseudomonas aeruginosa* bacteriophages. J. Bacteriol. **188:**1184–1187.
15. **Shen PS, Domek MJ, Sanz-Garcia E, Makaju A, Taylor RM, Hoggan R, Culumber MD, Oberg CJ, Breakwell DP, Prince JT, Belnap DM.** 2012. Sequence and structural characterization of Great Salt Lake bacteriophage CW02, a member of the T7-like supergroup. J. Virol. **86:**7907–7917.
16. **Iyer LM, Abhiman S, Maxwell Burroughs A, Aravind L.** 2009. Amidoligases with ATP-grasp, glutamine synthetase-like and acetyltransferase-like domains: synthesis of novel metabolites and peptide modifications of proteins. Mol. Biosyst. **5:**1636–1660.
17. **Ceyssens PJ, Hertveldt K, Ackermann HW, Noben JP, Demeke M, Volckaert G, Lavigne R.** 2008. The intron-containing genome of the lytic *Pseudomonas* phage LUZ24 resembles the temperate phage PaP3. Virology **377:**233–238.
18. **Doublie S, Tabor S, Long AM, Richardson CC, Ellenberger T.** 1998. Crystal structure of a bacteriophage T7 replication complex at 2.2 Å resolution. Nature **391:**251–258.
19. **Lane DJ.** 1991. 16S/23S rRNA sequencing, p 115–175. *In* Stackebrandt E, Goodfellow M (ed), Nucleic acid techniques in bacterial systematics. John Wiley & Sons, Inc, New York, NY.
20. **Brussaard CPD, Noordeloos AAM, Sandaa R-A, Heldal M, Bratbak G.** 2004. Discovery of a dsRNA virus infecting the marine photosynthetic protist *Micromonas pusilla*. Virology **319:**280–291.
21. **Hyman P, Abedon ST.** 2009. Practical methods for determining phage growth parameters. Methods Mol. Biol. **501:**175–202.
22. **Lin L, Han J, Ji X, Hong W, Huang L, Wei Y.** 2011. Isolation and characterization of a new bacteriophage MMP17 from *Meiothermus*. Extremophiles **15:**253–258.
23. **Lawrence JE, Steward GF.** 2010. Purification of viruses by centrifugation, p 166–181. *In* Wilhelm SW, Weinbauer MG, Suttle CA (ed), Manual of aquatic viral ecology. American Society of Limnology and Oceanography, Waco, TX.
24. **Steward GF, Culley AI.** 2010. Extraction and purification of nucleic acids from viruses, p 154–165. *In* Wilhelm SW, Weinbauer MG, Suttle CA (ed), Manual of aquatic viral ecology. American Society of Limnology and Oceanography, Waco, TX.
25. **Besemer J, Borodovsky M.** 1999. Heuristic approach to deriving models for gene finding. Nucleic Acids Res. **27:**3911–3920.
26. **Delcher AL, Harmon D, Kasif S, White O, Salzberg SL.** 1999. Improved microbial gene identification with GLIMMER. Nucleic Acids Res. **27:**4636–4641.
27. **Thomas JA, Rolando MR, Carroll CA, Shen PS, Belnap DM, Weintraub ST, Serwer P, Hardies SC.** 2008. Characterization of Pseudomonas chlororaphis myovirus 201ϕ2-1 via genomic sequencing, mass spectrometry, and electron microscopy. Virology **376:**330–338.
28. **Burge SW, Daub J, Eberhardt R, Tate J, Barquist L, Nawrocki EP, Eddy SR, Gardner PP, Bateman A.** 2013. Rfam 11.0: 10 years of RNA families. Nucleic Acids Res. **41:**D226–D232. doi:10.1093/nar/gks1005.
29. **Lowe TM, Eddy SR.** 1997. tRNAscan-SE: a program for improved detection of transfer RNA genes in genomic sequence. Nucleic Acids Res. **25:**955–964.
30. **Hughey R, Krogh A.** 1996. Hidden Markov models for sequence analysis: extension and analysis of the basic method. Comput. Appl. Biosci. **12:**95–107.
31. **Söding J.** 2005. Protein homology detection by HMM-HMM comparison. Bioinformatics **21:**951–960.
32. **Obeid S, Schnur A, Gloeckner C, Blatter N, Welte W, Diederichs K, Marx A.** 2011. Learning from directed evolution: *Thermus aquaticus* DNA polymerase mutants with translesion synthesis activity. Chembiochem **12:**1574–1580.
33. **Swofford DL.** 2002. PAUP*. Phylogenetic analysis using parsimony (* and other methods), version 4. Sinauer Associates, Sunderland, MA.
34. **Puck TT, Garen A, Cline J.** 1951. The mechanism of virus attachment to host cells. I. The role of ions in the primary reaction. J. Exp. Med. **93:**65–88.
35. **Lavigne R, Seto D, Mahadevan P, Ackermann HW, Kropinski AM.** 2008. Unifying classical and molecular taxonomic classification: analysis of the *Podoviridae* using BLASTP-based tools. Res. Microbiol. **159:**406–414.
36. **Summer EJ, Berry J, Tran TA, Niu L, Struck DK, Young R.** 2007. Rz/Rz1 lysis gene equivalents in phages of Gram-negative hosts. J. Mol. Biol. **373:**1098–1112.
37. **Filée J, Forterre P, Sen-Lin T, Laurent J.** 2002. Evolution of DNA polymerase families: evidences for multiple gene exchange between cellular and viral proteins. J. Mol. Evol. **54:**763–773.
38. **Lee YS, Kennedy WD, Yin YW.** 2009. Structural insight into processive human mitochondrial DNA synthesis and disease-related polymerase mutations. Cell **139:**312–324.
39. **Chan YW, Mohr R, Millard AD, Holmes AB, Larkum AW, Whitworth AL, Mann NH, Scanlan DJ, Hess WR, Clokie MR.** 2011. Discovery of cyanophage genomes which contain mitochondrial DNA polymerase. Mol. Biol. Evol. **28:**2269–2274.
40. **Sabehi G, Shaulov L, Silver DH, Yanai I, Harel A, Lindell D.** 2012. A novel lineage of myoviruses infecting cyanobacteria is widespread in the oceans. Proc. Natl. Acad. Sci. U. S. A. **109:**2037–2042.
41. **Kovalyova IV, Kropinski AM.** 2003. The complete genomic sequence of lytic bacteriophage gh-1 infecting Pseudomonas putida—evidence for close relationship to the T7 group. Virology **311:**305–315.
42. **Pope WH, Weigele PR, Chang J, Pedulla ML, Ford ME, Houtz JM, Jiang W, Chiu W, Hatfull GF, Hendrix RW, King J.** 2007. Genome sequence, structural proteins, and capsid organization of the cyanophage Syn5: a "horned" bacteriophage of marine synechococcus. J. Mol. Biol. **368:**966–981.
43. **Savalia D, Westblade LF, Goel M, Florens L, Kemp P, Akulenko N, Pavlova O, Padovan JC, Chait BT, Washburn MP, Ackermann HW, Hushegian A, Gabisonia T, Molineux I, Severinov K.** 2008. Genomic and proteomic analysis of ϕEco32, a novel *Escherichia coli* bacteriophage. J. Mol. Biol. **377:**774–789.
44. **Kropinski AM, Lingohr EJ, Ackermann H-W.** 2011. The genome sequence of enterobacterial phage 7-11, which possesses an unusually elongated head. Arch. Virol. **156:**149–151.
45. **Glukhov AS, Krutilina AI, Shlyapnikov MG, Severinov K, Lavysh D, Kocetkov VV, McGrath JW, de Leeuwe C, Shaburova OV, Krylov VN, Akulenko NV, Kulakov LA.** 2012. Genomic analysis of *Pseudomonas putida* phage tf with localized single-strand DNA interruptions. PLoS One **7:**e51163. doi:10.1371/journal.pone.0051163.
46. **Alemayehu D, Cassey PG, McAuliffe O, Guinane CM, Martin JG, Shanahan F, Coffey A, Ross RP, Hill C.** 2012. Bacteriophages φMR299-2 and φNH-4 can eliminate *Pseudomonas aeruginosa* in the murine lung and on cystic fibrosis lung airway cells. mBio **3**(2):e00029–12. doi:10.1128/mBio.00029-12.
47. **Tan Y, Zhang K, Rao X, Jin X, Huang J, Zhu J, Chen Z, Hu X, Shen X, Wang L, Hu F.** 2007. Whole genome sequencing of a novel temperate bacteriophage of *P. aeruginosa*: evidence of tRNA gene mediating integration of the phage genome into the host bacterial chromosome. Cell. Microbiol. **9:**479–491.
48. **Oakley AJ, Coggan M, Board PG.** 2010. Identification and characteriza-

tion of γ-glutamylamine cyclotransferase, an enzyme responsible for γ-glutamyl-ε-lysine catabolism. J. Biol. Chem. **285:**9642–9648.
49. **Llewellyn NM, Li Y, Spencer JB.** 2007. Biosynthesis of butirosin: transfer and deprotection of the unique amino acid side chain. Chem. Biol. **14:** 379–386.
50. **Mageeney C, Pope WH, Harrison M, Moran D, Cross T, Jacobs-Sera D, Hendrix RW, Dunbar D, Hatfull GF.** 2012. Mycobacteriophage Marvin: a new singleton phage with an unusual genome organization. J. Virol. **86:**4762–4775.
51. **Ivanova N, Daum C, Lang E, Abt B, Kopitz M, Saunders E, Lapidus A, Lucas S, Glavina Del Rio T, Nolan M, Tice H, Copeland A, Cheng JF, Chen F, Bruce D, Goodwin L, Pitluck S, Mavromatis K, Pati A, Mikhailova N, Bhen A, Palaniappan K, Land M, Hauser L, Chang YJ, Jeffries CD, Detter JC, Brettin T, Rohde M, Göker M, Bristow J, Markowitz V, Eisen JA, Hugenholtz P, Kyrpides NC, Klenk HP.** 2010. Complete genome sequence of *Haliangium ochraceum* type strain (SMP-2). Stand. Genomic Sci. **2:**96106. doi:10.4056/sigs.69.1277.
52. **Noble RT, Fuhrman JA.** 1997. Virus decay and its causes in coastal waters. Appl. Environ. Microbiol. **63:**77–83.
53. **Lovejoy C, Legendre L, Klein B, Tremblay J-E, Ingram RG, Therriault J-C.** 1996. Bacterial activity during early winter mixing (Gulf of St. Lawrence, Canada). Aquat. Microb. Ecol. **10:**1–13.
54. **Choi DH, Yang SR, Hong GH, Chung CS, Kim SH, Park JS, Cho BC.** 2005. Different interrelationships among phytoplankton, bacterial and environmental variables in dumping and reference areas in the East Sea. Aquat. Microb. Ecol. **41:**171–180.
55. **Ripp S, Miller RV.** 1997. The role of pseudolysogeny in bacteriophage-host interactions in natural freshwater environment. Microbiology **143:** 2065–2070.
56. **Cornelissen A, Ceyssens PJ, T'Syen J, Van Praet H, Noben JP, Shaburova OV, Krylov VN, Volckaert G, Lavigne R.** 2011. The T7-related *Pseudomonas putida* phage ϕ15 displays virion-associated biofilm degradation properties. PLoS One **19:**6:e18597. doi:10.1371/journal.pone.0018597.
57. **Lai SK, Hall DH.** 1993. A novel approach for isolation and mapping of intron mutations in a ribonucleotide reductase encoding gene (nrdB) of bacteriophage T4 using the white halo plaque phenotype. Biochem. Biophys. Res. Commun. **196:**943–949.
58. **Moussa SH, Kuznetsov V, Tran TA, Sacchettini JC, Young R.** 2012. Protein determinants of phage T4 lysis inhibition. Protein Sci. **21:**571–582.
59. **Hyman P, Abedon ST.** 2010. Bacteriophage host range and bacterial resistance. Adv. Appl. Microbiol. **70:**217–248.